Infrared Laser Spectroscopy of Imidazole Complexes in Helium Nanodroplets: Monomer, Dimer, and Binary Water Complexes

Myong Yong Choi* and Roger E. Miller†

Department of Chemistry, The University of North Carolina at Chapel Hill, Chapel Hill, North Carolina 27599

Received: April 19, 2006; In Final Form: May 30, 2006

Infrared laser spectroscopy has been used to characterize imidazole (IM), imidazole dimer (IMD), and imidazole−water (IMW) binary systems formed in helium nanodroplets. The experimental results are compared with ab initio calculations reported here. Vibrational transition moment angles provide conclusive assignments for the various complexes studied here, including IM, one isomer of IMD, and two isomers of the IMW binary complexes.

Introduction

Recently, the first structure of a neutral ammonia channel from a bacterial membrane was determined, providing considerable insight into the process of neutral gas transport in membranes.[1,2] The structure shows that the hydrogen-bonding network between the imidazole (IM) moiety of the histidine and ammonia molecules in the channel plays an important role in neutral ammonia gas transport through the membrane. Not only is the intermolecular interaction between IM and ammonia important, but the self-associating interaction of IM, i.e., the IM dimer (IMD), also plays an important role in the hydrogen-bonding networks of the ammonia channel. Due to the unique IM structure, which contains a proton donor N−H and a proton acceptor N atom, IMD has been extensively studied as a model system both theoretically[3−7] and experimentally.[8−11]

Understanding the intermolecular interaction of IM−water complexes is also relevant owing to their importance in hydrated biological systems such as histidine residue[12] and hydrated nucleic acid base (NAB) complexes.[13−17] Indeed, the location and orientation of individual water molecules in the binary complexes play a pivotal role in some other biological processes. For example, water-assisted proton transfer in guanine[18− 20] and cytosine[21− 23] involve a single water molecule that forms a double hydrogen bond which bridges the proton donor and proton acceptor sites in the molecule.

Many theoretical[24−27] and experimental[11,28,29] investigations have been devoted to the structures and relative energies of IM−water (IMW) complexes due to the occurrence of the IM five-membered ring in adenine and guanine. Ab initio calculations have consistently shown that the two isomers, >NH···OH_2 (IMW1) and >N:···H−O−H (IMW2) (see Figure 1), have almost the same energy. Infrared spectroscopy was used to study the hydrogen-bond interaction of the two isomers of the IM−water complex by matrix-isolation FTIR spectroscopy.[28] However, to our knowledge, no gas-phase vibrational study of IM−water complexes has been previously reported. Recently, the IM derivatives 4/5-phenyl IM, complexes with a single water, were studied by IR ion dip spectroscopy,[12,30] which suggested the presence of only one isomer, > N: ···H−O−H, out of the three predicted ones.

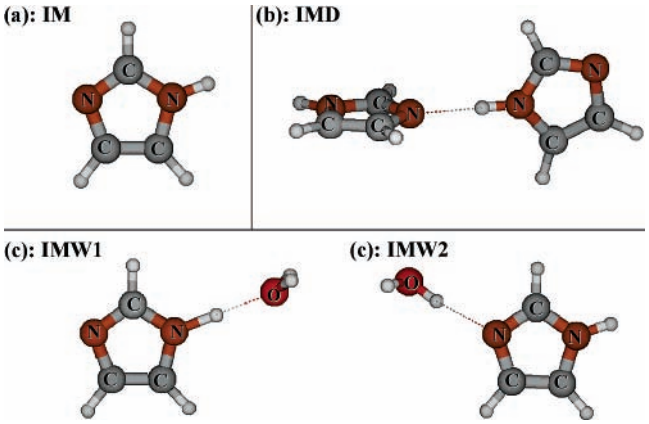

Figure 1. (a) Imidazole monomer (IM), (b) global minimum of imidazole dimer (IMD), and (c) two isomers of imidazole water binary complexes (IMW1 and IMW2).

Our approach in this study involves the use of helium nanodroplets, which has been shown to be an ideal matrix for infrared spectroscopy.[31−35] The weak interactions between the helium and the molecules of interest give rise to small vibrational frequency shifts (within a few wavenumbers) and high spectral resolution due to ultra cold helium nanodroplets (0.37K).[32,36] In a recent paper[13] we reported on a combined experimental/theoretical study of all four of the theoretically predicted isomers of uracil−water using infrared laser spectroscopy in helium nanodroplets, which revealed the conformational energy landscapes of those hydrated complexes. We assigned closely spaced vibrational bands by experimentally measuring the angles between the vibrational transition moments and the permanent dipole moment of the molecule for the associated vibrational modes.[13,37,38] These vibrational transition moment angles (VTMAs) also provide detailed structural information on the species of interest. Determination of these quantities is accomplished by orienting the molecule in a large DC electric field[39−42] and measuring the integrated intensities of the vibrational bands as a function of the laser polarization direction. For the case of well-isolated, high-frequency X−H stretches, we find that these angles can be reliably calculated using conventional ab initio methods based upon harmonic frequency calculations.[43] Indeed, these angles are much less sensitive to the detailed multidimensional potential surface but

* To whom correspondence should be addressed. E-mail: mychois@unc.edu.

† Deceased November 6, 2005.

10.1021/jp0624146 CCC: $33.50
Published on Web 07/08/2006

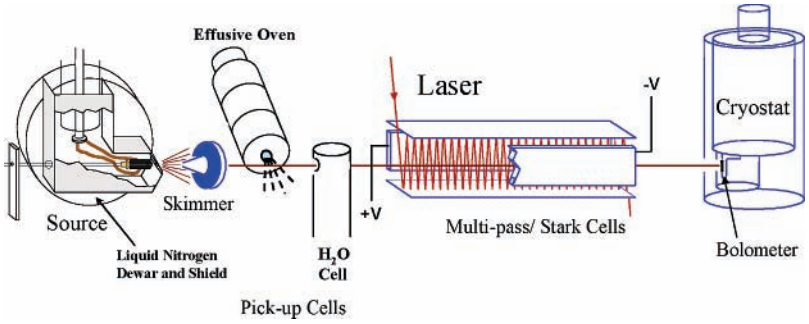

Figure 2. Schematic diagram of the experimental apparatus used in the present study. An effusive oven was used. A bolometer was used to monitor laser-induced depletion helium droplet beam intensity.

rather depend primarily on the structure of the molecule, particularly for its high-frequency modes. The sensitivity of the method to the molecular structure was first demonstrated for adenine, where the experimental VTMAs for the N−H and NH_2 stretches were highly dependent upon the out-of-plane NH_2 tilt angle.[43] In the present study we apply this method to report on the isomers of the IM−water binary complexes (IMW) and the IM dimer (IMD) (see Figure 1) in helium nanodroplets.

Experimental Section

The helium droplet apparatus has been previously described[44] and is illustrated in Figure 2. In the present study the nanodroplets pass within 2 mm of the exit of the oven producing a low vapor pressure (between 10^{-6} and 10^{-5} Torr) of IM (Aldrich, 99% purity). Collisions between the gas-phase molecules and the droplets result in solvation of the former by the latter. The vapor pressure at the exit of the oven can be varied to pick up the desired number of IM molecules, according to the associated Poisson statistics.[45] In practice, useful operating temperatures for IM were from 25 to 35 °C with our effusive pick-up cell oven. To maximize the pick up of molecules into the helium nanodroplets at a minimum heating temperature, we developed a pick-up oven through which the helium droplets entered and exited via 2 mm holes.[46−48] However, because of the high IM vapor pressure, this oven resulted in the pick up of too many molecules. We thus constructed a new effusive oven, shown in Figure 2, which was less efficient and thus solved this problem. In detail, the tip of the effusive oven, a 1 mm diameter hole, faces the droplet beam axis. The end of the oven is positioned just below the helium nanodroplet beams, and the droplets pass by and pick up the target molecules at the exit of the effusive oven. A second pick-up cell was positioned downstream of the oven in order to add water to the droplets. Because of the high mobility of molecules in the helium droplets, all molecules added to the droplets end up in a complex, located close to the middle of the droplet. This is based on the fact that most molecules are solvated by liquid helium rather than by "vacuum". Notable exceptions are the alkali atoms which reside on the surface of the droplets due to their weaker interactions with helium atoms than the He−He interactions.[49−52]

Once the species of interest are formed, the doped nanodroplets pass between the plates of a multipass/Stark cell,[44] which is used to generate many crossings between the infrared laser and the helium nanodroplet beam. The result is efficient vibrational excitation of the solvated molecules. A large DC electric field can also be applied to the interaction region for the purposes of orienting the molecules in the laboratory frame of reference. This was done in order to measure the vibrational transition moment angles of the various species, as discussed below. All of the spectra reported here were obtained using a periodically poled lithium niobate (PPLN) cw-OPO[53,54] from Linos Photonics (70 mW output power in the region of interest). Several external etalons and a wavemeter were used to calibrate the spectra reported here.

The pendular state method used to orient the molecules of interest has been applied previously to both gas-phase[55−59] and helium nanodroplet[35,40−42,59] studies. A large DC electric field results in the orientation of the permanent dipole moment of the target molecules (e.g., IM, IMD, and IMW complexes) parallel to the electric field in the limit where μE is large compared to the rotational temperature (in this case 0.37 K[32,36]). For a linearly polarized laser the result will be a change in the excitation efficiency given that the molecular transition moments will also be oriented in the laboratory frame of reference. If the laser electric field is aligned parallel (perpendicular) to the DC electric field (referred to here as parallel and perpendicular polarization alignments) the corresponding change in the vibrational band intensity will depend on the angle between the permanent dipole axis and the corresponding transition moment direction. This angle is referred to here as the vibrational transition moment angle or VTMA. For a vibrational mode with its transition moment parallel to the permanent dipole moment, parallel (perpendicular) polarization will result in a significant increase (decrease) in the band intensity compared to the zero-field case.

A quantitative description of this effect requires that the orientation distribution for the permanent dipole moment be known. This distribution depends on the magnitude of the dipole moment, applied electric field, rotational constants, and temperature of the molecule in question. The methods for calculating these distributions have been discussed in detail previously.[60−63] For the IM monomer the partially resolved rotational structure is observed in the zero field. For the other systems discussed herein, the experimental spectra are broadened to a Lorentzian line shape. Although this means that the rotational constants cannot be directly determined from the experimental spectra, it also means that the overall orientation distribution is less sensitive to the rotational constants. In this case we used the ab initio rotational constants, divided by a factor of 3 to account for the effects of the helium,[64] to determine the orientation distribution needed to calculate the VTMAs. This approach works rather well given that the rotational temperature of the droplets, and hence the rotational temperature of the molecules, is well known, namely, 0.37 K. A detailed discussion of how the experimental VTMAs are extracted from the integrated areas of the zero field and parallel and perpendicular polarization spectra is given elsewhere.[13,37,38,43,65] The experimental VTMAs can be compared directly with those obtained from ab initio calculations, carried out using Gaussian 03.[66] The calculations reported here were all carried out at the MP2 level with a

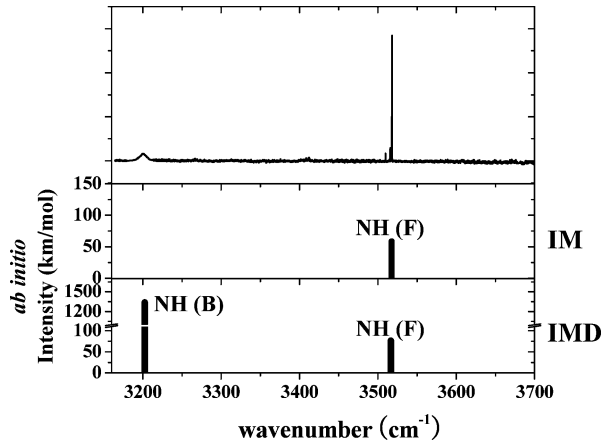

Figure 3. Survey spectrum of imidazole monomer (IM) and dimer (IMD) isolated in helium droplets. The corresponding ab initio vibrational spectra for IM (scaled by a factor of 0.9556 with 6-311++G(d,p) basis set) and the IMD (scaled by a factor of 0.957 with 6-311+G(d) basis set) are shown below the experimental spectrum.

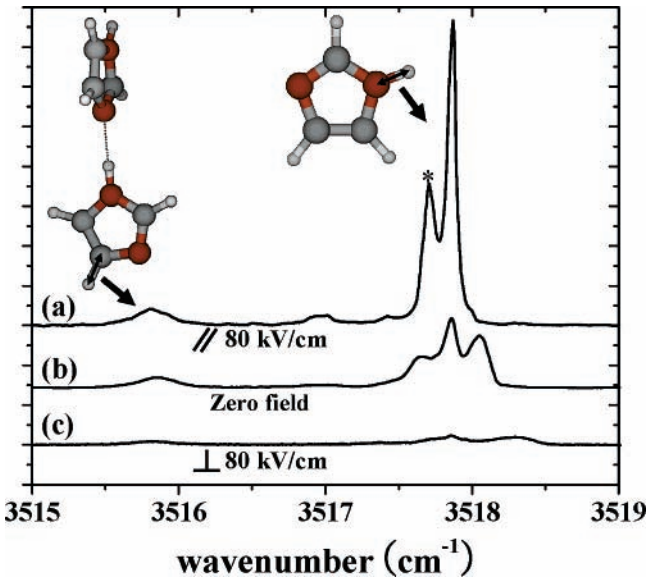

Figure 4. Expanded view of the N−H stretch of the IM monomer and dimer. Spectra a, b, and c correspond to parallel polarization, zero field, and perpendicular polarization (the corresponding electric field being 80 kV/cm), respectively. The assignments shown in the figure are based upon comparisons in VTMAs and frequencies between the experimental and ab initio values. The origin of the band marked with an asterisk is not clearly known at this time.

6-311++G(d,p) basis set except for IMD where a 6-311+G(d) basis set is used.

Results and Discussion

Imidazole Monomer and Dimer. We begin this discussion by considering the case where the water vapor pick-up cell is left empty, so that only the IM monomer or the associated complexes are formed in the droplets. The upper panel in Figure 3 shows an experimental spectrum of IM and an isomer of IMD in helium nanodroplets that spans the regions corresponding to the free N−H and bonded N−H stretching vibrations. The survey spectrum was recorded at rather low oven temperatures, so that the monomer and the self-associated dimer are the only species formed. The middle panel shows the ab initio spectra (frequencies scaled by a factor of 0.9556 with a 6-311++G-(d,p) basis set) for the IM monomer, and the bottom panel shows those of the global minimum structure of IMD scaled by a factor of 0.957 with a 6-311+G(d) basis set. (The energetics and ab initio calculations for the isomers of IMD will be discussed as below.) The largest peak in the spectrum is easily assigned to the N−H stretching vibration of the IM monomer at 3517.8 cm^{-1}. Two additional bands observed in the spectrum and indicated in the figure are assigned to the IMD. Figure 4 shows an expanded view of the region corresponding to the free N−H stretches of the monomer and dimer, also showing the effect of applying a DC electric field with different polarization directions: (a) parallel polarization, (b) zero electric field, and (c) perpendicular polarization (the corresponding electric field being 80 kV/cm). The zero-field spectrum of the IM monomer shows partially resolved rotational fine structure in the form of a PQR contour. The observed vibrational origin and the corresponding ab initio values are listed in Table 1.

It is immediately obvious from the polarization dependence of the N−H stretch of the IM monomer in Figure 4 that this band is approximately parallel (VTMA close to 0°). This is consistent with the ab initio calculation of the VTMA for this mode, namely, 18° (see Table 1.) The experimental determination of this quantity requires inclusion of all of the rotational states given that the band is partially rotationally resolved. The origin of the peak marked with an asterisk in parallel polarization is not known at this moment.

The weaker band near 3515.8 cm^{-1} is tentatively assigned to the IMD, based upon the pick-up oven temperature dependence of the associated signals. Here again we find that the band is enhanced by application of a DC electric field in parallel polarization. A detailed analysis of the associated integrated intensities yields a VTMA for this band of 33°. The ab initio VTMA for the free N−H mode of the IMD is 30°, in good agreement with the experimental result. The small frequency shift associated with this band (from the IM monomer) indicates that this is a "free" N−H vibrational mode in the dimer. We carried out extensive ab initio calculations on the four lowest energy dimers (figure shown in the Supporting Information) using the MP2 level with a 6-311+G(d) basis set. The relative energies are 17, 22, and 27 kJ/mol (with zero-point energy corrections) higher than the global minimum. The global minimum is the "twisted" hydrogen-bonded complex, shown in Figure 1, which has strong intermolecular N···H−N hydrogen bonds, while the three higher energy isomers have weaker N···H−C hydrogen bonds. It is worth mentioning here that the structure of this twisted hydrogen-bonded complex (IMD) is very similar to the structure of the hydrogen-bond IM complex (at the histidine residue) in the ammonia channel[1,2] mentioned above.

A summary of the ab initio results for all four isomers is given in the Supporting Information. Although all of these isomers have "free" N−H vibrational bonds, it is interesting to note that only the global minimum structure gives a VTMA for the "free" N−H stretch that is in agreement with experiment. As shown in the Supporting Information, the VTMAs of the "free" N−H stretches for the three higher energy dimers vary from 50° to 90°, which is very different from that of the global minimum dimer (IMD), 33°. It is also interesting to note that this is the most polar structure, which is also consistent with the fact that the observed spectrum is strongly dependent upon application of a DC electric field.

The "twisted" hydrogen-bonded dimer complex is the only one that shows a strongly shifted N−H vibrational mode. As a result, further evidence for formation of this isomer can be obtained through probing the corresponding spectrum. Figure 5

TABLE 1: Summary of the Experimental and ab Initio Data for the Imidazole Monomer (IM), Imidazole Dimer (IMD), and Two Lowest Energy Isomers of Imidazole−Water Binary Complex (IMW1 and IMW2)

	harm.[a] freq. (cm^{-1})	scaled[b] freq. (cm^{-1})	exp. freq. (cm^{-1})	IR. intensity (km/mol)	assignment	ab initio VTMAs (deg)	exp. VTMAs (deg)	dipole moment (D)	relative[c] energy (kJ/mol)
IM	3681.3	3517.9	3517.9	77.7	NH (F)	18	parallel	3.97	
IMD								9.62	
	3673.8	3515.8	3515.8	81.6	NH (F)	30	33		
	3388.0	3242.3	3200.1	1225.3	NH (B)	10	20		
IMW1								6.67	0.0
	3988.5	3811.4	3747.7	99.6	OH (AS)	90	90		
	3870.5	3698.7		22.6	OH (SS)	26			
	3560.2	3402.1	3411.8	568.1	NH (B)	6	22 (10)[d]		
IMW2								5.72	0.5
	3959.6	3783.8	3719.7	84.0	OH (F)	33	33		
	3678.8	3515.5	3517.8	46.9	NH (F)	76	perpendicular		
	3668.5	3505.6	3447.9	763.3	OH (B)	12	27		

[a] The ab initio calculations were performed at the MP2/6-311++G(d,p) level (for IMD a 6-311+G(d) basis set was used). [b] The scaled frequencies were obtained by multiplying the harmonic frequencies by a factor of 0.9556 to account for the effects of anharmonicity (for IMD a factor of 0.957 was used). [c] The energy was obtained with zero-point energy correction. [d] The experimental VTMA for the bonded NH band for IMW1 parentheses was obtained from deuterium substitution.

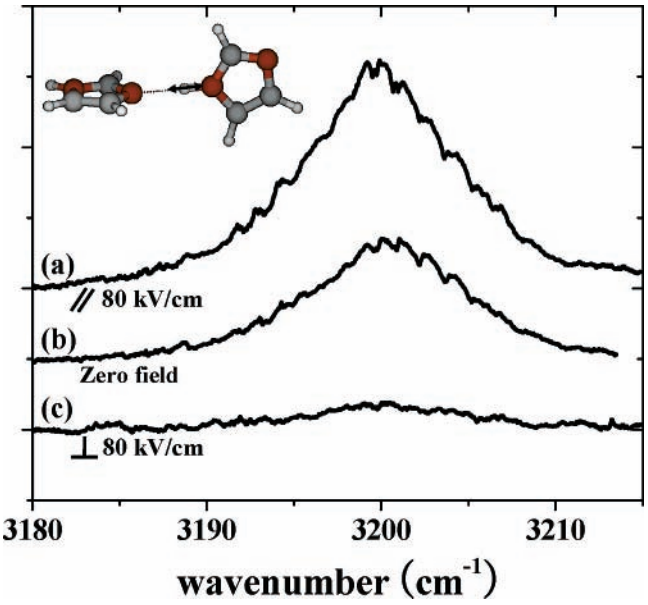

Figure 5. Expanded view of the bonded N−H stretch of the IMD. Spectra a, b, and c were recorded with parallel polarization, zero field, and perpendicular polarization conditions, respectively.

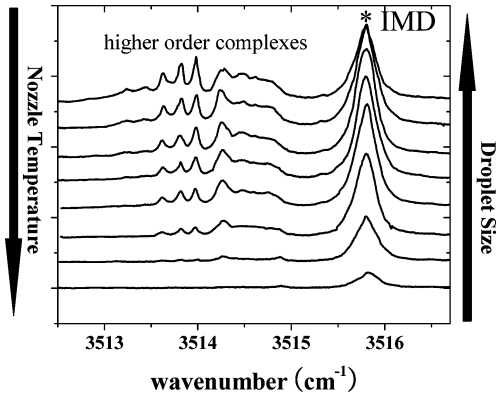

Figure 6. Evolution of the spectra for different nozzle temperatures (top to bottom 15, 17.5, 18.5, 19.5, 20.5, 21.5, 23, and 25 K). The band marked with an asterisk is the free N−H stretch of imidazole dimer.

shows a scan of a spectrum which has the same oven temperature dependence as the dimer band observed in the "free" N−H stretching region. We assign this band to the bonded NH stretching mode. Detailed analysis of the polarization dependence of this band reveals an experimental VTMA of 20°, which is less parallel than the ab initio value of 10°. The difference, which is a bit larger than what we have seen for other bands, probably results from the increased error in determining experimental VTMAs when the angle is small, e.g., below 15°.[67] Assignment of this band to the bonded N−H stretch of IMD is further supported below. Note that the line width of this band is in excess of 10 cm^{-1} and the experimental frequency shift from the free N−H stretch is almost 316 cm^{-1}, which is slightly larger than the ab initio calculation value of 274 cm^{-1}. It is evident that the band is associated with a strong hydrogen bond, based on the magnitude of the frequency red shift and peak broadening. Such a broad band associated with a hydrogen bond was previously observed in the indole−water system by Zwier and co-workers[68] and could come from the dipole−induced dipole interactions.[69,70] A recent paper by Sibert et al.[71] provides a theoretical model for the band broadening. It is interesting to note that the total integrated area under the zero-field spectrum is about 16 times larger than that of the corresponding "free" N−H stretch. This is also in good agreement with the ratio of the corresponding ab initio intensities, namely, 15 times (see Table 1). In conclusion, it is quite clear that the only isomer of the IMD that is formed in helium nanodroplets is the one corresponding to the global minimum on the potential energy surface. This is also the structure that corresponds to the dipole-oriented structure that we have come to expect to form from highly polar, moderately heavy molecules in helium nanodroplets.[48]

Formation of linear chains of polar molecules in helium is well established from previous studies carried out in our laboratory.[35,72] The reason for this is the sequential addition of monomer units to existing chains, beginning with the dimer, whose structure is trapped in its potential well in the low-temperature helium environment. It is therefore interesting to consider the series of spectra shown in Figure 6, obtained as a function of the nozzle temperature and hence the mean droplet size. Large droplets have large cross sections and sufficiently high heat capacities to capture and cool many IM molecules. The rather smooth evolution of the spectra corresponding to the "free" N−H stretches suggests formation of chains. We have,

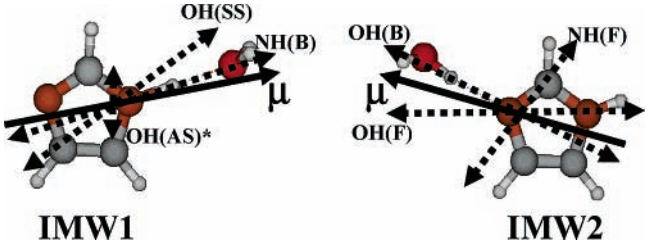

Figure 7. Two lowest energy isomers of imidazole−water binary complexes (IMW1 and IMW2) showing the corresponding directions of the permanent electric dipole moments (solid arrows) and the vibrational transition moments (dashed double-ended arrows) for the various vibrational modes. Note that the vibrational transition dipole moment of OH (AS) marked with an asterisk is out of plane, so that the VTMA of this band is 90°. The magnitudes of these moments are given in Table 1.

however, not analyzed these peaks in any detail. Nevertheless, formation of such linear chains is interesting in its own right given that the IMD molecule has an inherent 30° bend in the monomer unit.

Imidazole−Water Complexes. We now turn our attention to the binary complexes of IM with water (IMW). Two hydrogen-bonded isomers of the IMW binary complex (>NH···OH_2 and >N:···H−O−H, see Figure 1) are presented here. The two isomers were formed by sequential pick-up of one IM and one water molecule by helium droplets. Figure 7 shows the two lowest energy ab initio structures for the IMW binary system onto which are superimposed vectors representing the directions of the permanent electric dipole moments (solid arrows) and the vibrational transition moments (dashed arrows). The magnitudes of the various moments are given in Table 1. It is clear from the figure that the pattern of VTMAs for the two isomers is quite different, making them a useful tool for distinguishing these two isomers and assigning the associated vibrational spectra.

The lowest energy form (IMW1) corresponds to the water acting as a proton acceptor, while the slightly higher energy form (IMW2) has the water donating a proton to the nitrogen atom in the IM ring. The spectrum a upper panel, shown in Figure 8, in which the water source was closed, shows that only IM monomer and dimer are present in the helium droplets. The rich spectrum b is obtained by optimizing the pick-up conditions for the capture of a single IM molecule and one water molecule; therefore, the additional peaks in b must involve H_2O. The dotted lines are meant as guides to associate the bands with their calculated frequencies. The ab initio frequency calculations for the two isomers are summarized in the bottom panels of Figure 8 in which we used a single scaling factor of 0.9556 for all of the vibrational modes. This gives good agreement between theory and experiment for the free N−H stretches. Although this single scaling factor gives rather poor agreement for the case of the free and bonded O−H stretches,[13,37,38] the experimental frequency difference (278.3 cm^{-1}) between the free and bonded O−H stretches is in good agreement with the ab initio calculations (271.8 cm^{-1}). Once again, the relative integrated intensities (corrected with ab initio intensities) of bonded N−H and O−H bands (see Table 1) are almost 1:1, thereby suggesting that the relative abundance of the two isomers is similar.

The other bands in Figure 8 may be associated with higher order clusters. Although the water pressure is optimized for binary complexes, the pick-up of more than one water molecule by the droplets is still significant under these conditions, and some of the peaks in the spectrum are due to complexes containing three molecules (IMD plus water or IM plus two waters).

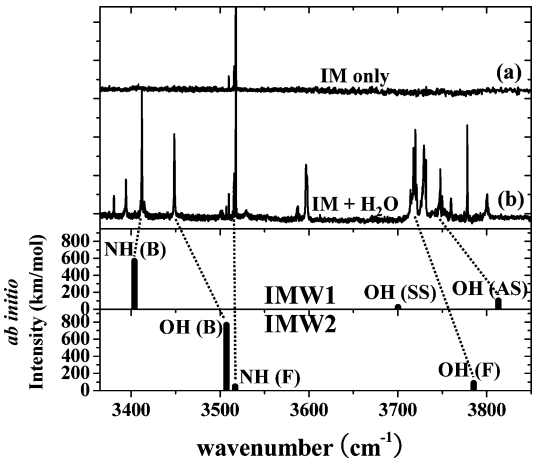

Figure 8. Survey spectrum of IM (a) without and (b) with water isolated in helium droplets. The ab initio frequency calculations for the corresponding isomers, IMW1 and IMW2 (scaled by a factor of 0.9556 with 6-311++G(d,p) basis set), are shown below the experimental spectra. The dotted lines are meant as a guide to assign the bands associated with calculated frequencies of the IM + H_2O complexes (IMW1 and 2). The other bands in b, not matched with dotted lines, are due to higher order complexes of IM and water molecules (see text for details).

However, discussion of the latter species is beyond the scope of the present study.

We now proceed to consider the assignment of the high-frequency portion of the spectrum appearing in the region near 3730 cm^{-1}, corresponding to the free O−H stretches of the water molecule. Figure 9 shows this region measured with (a) parallel polarization, (b) zero electric field, and (c) perpendicular polarization (the corresponding electric field being 80 kV/cm). The peaks labeled as "w" are due to water monomer and high-order water clusters ($(H_2O)_{1-2}$). Examination of the oven temperature dependence and water pick-up pressure dependence of the various peaks in this region of the spectrum reveals that only bands i and ii are due to the IM−water binary system, namely, asymmetric stretch mode (OH (AS)) of IMW1 and free O−H stretch mode (OH (F)) of IMW2. The symmetric O−H stretch of IMW1 was not observed in the region below 3700−3600 cm^{-1}, which is not surprising given that the expected band intensity is much weaker (see Table 1). Nevertheless, a number of scans were taken in order to convince us that there is no band in this region of the spectrum. It is also not observed in the study of H_2O in helium droplets.[73] The remaining peaks in the spectrum are all uniquely assigned to other species and will be discussed in detail elsewhere.[74]

It is evident from the polarization dependence of the two IM−water bands that the one appearing at lower frequency is nearly parallel while the higher frequency mode completely disappears with parallel polarization. Analysis of these bands, based upon fitting to Lorentzian line shapes, yielded VTMAs for these two bands of 33° (ii) and 90° (i). For comparison, the ab initio VTMAs for the two isomers are 33° and 90° for the "free" O−H stretch (ii) of IMW2 and the asymmetric stretch (i) of IMW1, respectively. The agreement between experiment and theory is clearly excellent. It is interesting to note that the frequency difference (28.0 cm^{-1}) is in excellent agreement with the ab initio calculations (27.6 cm^{-1}) even though the absolute scaled frequencies are not as well reproduced especially for free O−H stretches.[13,37,38] The relative integrated intensity ratio of i and ii bands (see Table 1) is 1:1, consistent with the expected ratio populations of these two nearly equal energy isomers.

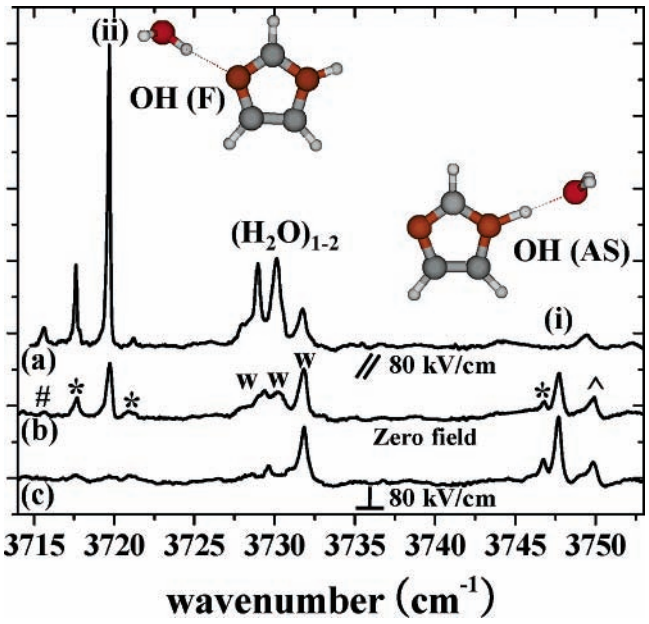

Figure 9. Expanded view of the high-frequency section (OH (AS) and OH (F)) of the IM−water complex spectrum. Infrared spectra a, b, and c correspond to parallel polarization, zero field, and perpendicular polarization, respectively. The higher frequency band (i) corresponds to the OH (AS) stretch mode of IMW1, while the lower frequency band (ii) is associated with the OH (F) stretch mode of IMW2. The bands marked with an asterisk are due to IM monomer with two water molecules determined by water pressure dependence experiments. The band marked with "#" and "∧" is due to IMD with one water molecule determined by IM temperature dependence experiments and water−nitrogen complexes, respectively. The bands marked with "w" are related to pure water complexes.

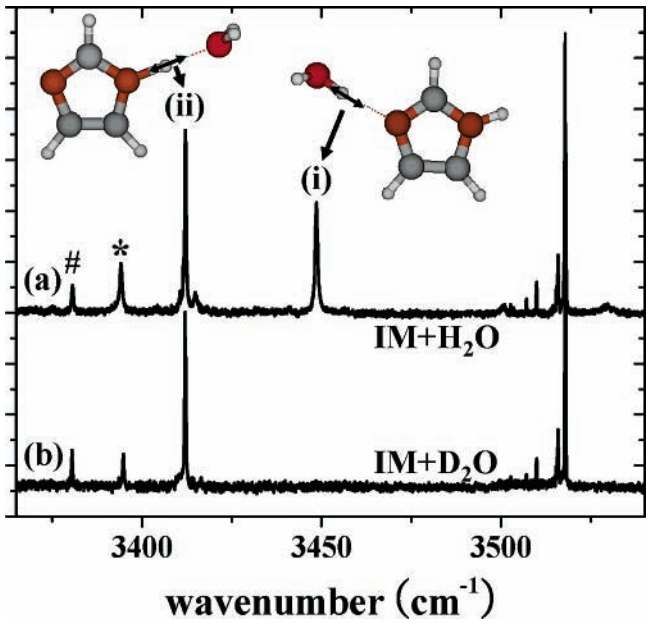

Figure 10. Comparison of spectra of the bonded O−H and N−H stretching region obtained using both H_2O (a) and D_2O (b). The higher frequency band (i) corresponds to the bonded O−H stretch mode of IMW2, while the lower frequency band (ii) is associated with the bonded N−H stretch mode of IMW1. The bands marked with an asterisk are due to IM monomer with two water molecules determined by water pressure dependence experiments. The bands marked with "#" are due to IMD with one water molecule determined by IM temperature dependence experiments.

We now turn our attention to the bonded vibrations of the IM−water binary system, which appear in the region from 3400 to 3500 cm^{-1}. Given the structures shown in Figure 7, we expect to see a bonded N−H vibrational mode for IMW1 and a bonded O−H stretch for IMW2. Figure 10 shows a comparison of spectra obtained using both H_2O and D_2O. The disappearance of the peak at 3450 cm^{-1} upon deuteration identifies it as a bonded OH band. Its complete disappearance also confirms a previous result[13] that there is no isotopic scrambling in these helium nanodroplet experiments. We conclude that the vibrational band i is associated with the bonded O−H stretch of IMW2. From the oven temperature and water pressure dependence of the peaks in this spectrum we can also conclude that the only peaks that correspond to the binary complex are bands i and ii. As a result, we assign bands i and ii to the bonded O−H stretch of IMW2 and the bonded N−H stretch of IMW1, respectively. The remainder of the peaks in the spectrum are due to either the IM monomer and dimer (discussed above) or higher order complexes that will be discussed in detail elsewhere.[74]

Figure 11 shows the electric field dependence of the two bands discussed above from which the VTMAs are determined for the bonded N−H stretch of IMW1 (22°) and the bonded O−H stretch of IMW2 (27°). In these cases, agreement with the ab initio VTMAs of 6° and 12° is poor. These two bands are very close to being pure parallel bands (below 15°)[67] for which the experimental VTMAs give larger errors as mentioned above. Nevertheless, this error is well outside the experimental uncertainty that we have come to expect, leading us to consider other explanations for the differences. Since we are confident in the assignment of these two bands, we are forced to consider other mechanisms that might affect this comparison. One possibility is that there are other bands that overlap with these bands which would affect the corresponding experimental results. Another is that these complexes are rather floppy, so that the ab initio results for the equilibrium geometry are not sufficient.

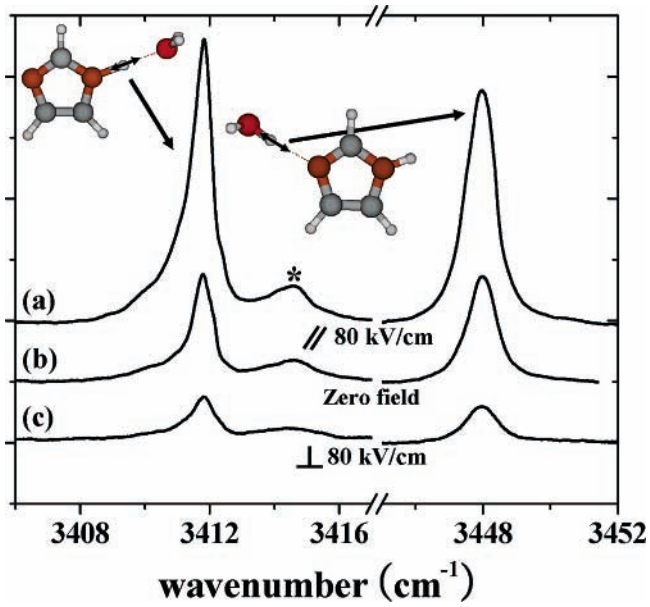

Figure 11. Expanded spectra of the bonded O−H and N−H stretching region. Spectra a, b, and c were recorded parallel polarization, zero field, and perpendicular polarization conditions, respectively. The band marked with an asterisk is assigned to IM complexes containing more than one water molecule.

To test these ideas we also obtained VTMAs for the bonded NH vibrational bands in the IM−D_2O complex. The data for

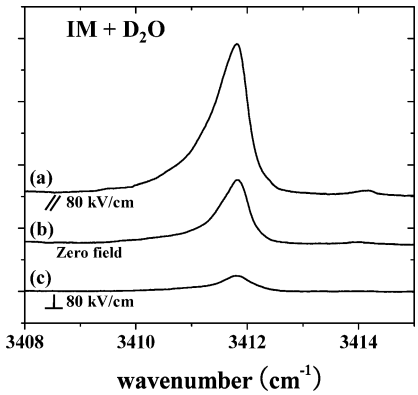

Figure 12. Expanded spectra of the bonded N−H stretch mode of the IM−D_2O complex. Spectra a, b, and c were recorded parallel polarization, zero field, and perpendicular polarization conditions, respectively.

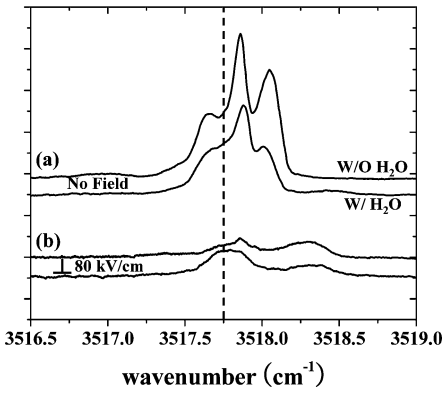

Figure 13. Comparison between the free N−H stretch region without (upper) and with (below) water added to the droplets. Spectra a and b were recorded zero field and perpendicular polarization conditions, respectively. The vapor pressure of water was 9×10^{-7} Torr at the pick up cell.

this band are shown in Figure 12. In this case, the experimental VTMA is determined to be 10°, in much better agreement with the ab initio value of 6°. Unfortunately, we are not able to conclusively decide which of the above effects is responsible for the large difference between the water and deuterium results. Indeed, there could be an O−H band from some other species present in the droplet that overlaps with the bonded N−H vibration when water is used, which disappears when using D_2O, or alternatively the heavier mass of the deuterium could reduce the wide amplitude motion and thus give better agreement with the ab initio results. The fact that the agreement in the free O−H region is so good leads us to believe that the problem is the former rather than the latter. This is somewhat supported by the fact that the spectrum is much smoother in the IM−D_2O spectrum, in comparison to that of IM−H_2O, which might indicate that there are overlapping bands in the H_2O case. Theoretical studies of the wide amplitude motions in these binary complexes will be needed to clarify this issue.

Finally, we consider the free N−H stretch of IMW2, which should also be visible in the spectral region of interest here. Unfortunately, this vibrational band is expected to be only slightly shifted from the very intense vibration band of the IM monomer and weaker as well, making it difficult to observe. However, as indicated in Table 1, the free N−H band of IMW2 is predicted by theory to be a nearly perpendicular band (VTMA = 76°), while the monomer band is nearly parallel. To confirm that this band exists in the spectrum, we took advantage of this difference and used a perpendicular polarization geometry to eliminate the monomer from the spectrum while at the same time enhancing the contribution from the IM−water complex. Figure 13 shows the spectra in the free N−H stretch region, recorded with (a) no applied field and (b) an applied DC electric field directed perpendicular to the laser polarization direction and a comparison between the experimental results with and without water added to the droplets. The water pressure at the pick-up cell was up to 9×10^{-7} Torr, which is very low compared to that of the optimum condition for one water (2.4×10^{-6} Torr), to make sure that the band comes from only the IM with one water complex. The vertical dashed line shows that there is a perpendicular band underneath the monomer band at about 3517.8 cm^{-1} that is evident only when the water is present. Although this enables us to identify this band, we are unable to report a VTMA for this band because the corresponding zero-field and parallel polarization spectra could not be obtained. The data are nevertheless sufficient to confirm that this band is nearly perpendicular, as reported in Table 1.

It is clear from the above results that both IMW1 and IMW2 are formed in helium nanodroplets, consistent with the idea that the water approaches from a random direction and then gets trapped in the nearest minimum on the potential energy surface that is separated from the other by a sufficiently high barrier to prevent rearrangement.

Conclusions and Future Work

In this combined experimental/theoretical study we report high-resolution infrared laser spectra of imidazole (IM), imidazole dimer (IMD), and two isomers of imidazole water complexes (IMWs) isolated in helium nanodroplets. For IM monomer and dimer, the calculated frequencies are very well matched with the observed frequencies. By orienting the molecules with a strong DC electric field, we achieved a definitive assignment for the IMD using the vibrational transition moment angles (VTMAs). For the case of the IM−water binary complexes, as shown in Figure 8, the calculated frequencies of the bonded O−H and asymmetric stretches are in poor agreement with the observed frequencies. However, an unambiguous assignment of the above bands is achieved with the aid of the VTMAs and deuterium substitution for the binary complexes.

The relative abundances of the two isomers, IMW1 and IMW2, are found to be almost 1:1, which could be the result of both energetic and dynamical effects associated with the formation of the clusters in the helium. In particular, formation of the two IMW complexes in almost equal population could be ascribed to their almost identical relative energies and the equal widths of the entrance valley (funnel) where a water molecule can be trapped by the long-range potential energy surface.

The studies of IMW complexes are of help in the characterization of the experimental spectra of adenine− and guanine−water complexes, which we plan to study. We are currently carrying out studies of higher order IM−water complexes, such as IM + two waters (IM2W) and IMD + one water (IMDW) complexes,[74] which would provide further fundamental understanding of hydrogen-bonding effects associated with IMD in the ammonia channel. Nevertheless, in future studies we also plan to investigate the IM−ammonia complex, which is directly related to the mechanism of the ammonia gas transport in physiological conditions.

Acknowledgment. Support for this work from the National Science Foundation (CHE-04-46594) is gratefully acknowledged. M.Y.C. thanks Prof. Tomas Baer for advice in this paper.

Supporting Information Available: Figure of the four lowest energy IM dimers (IMD, IMD1, IMD2, and IMD3), energies and optimized geometries of the four IMDs, and summary of the experimental and ab initio data for the four IMDs. This material is available free of charge via the Internet at http://pubs.acs.org.

References and Notes

(1) Khademi, S.; O'Connell, J., III; Remis, J.; Robles-Colmenares, Y.; Miercke Larry, J. W.; Stroud, R. M. *Science* **2004**, *305*, 1587.

(2) Zheng, L.; Kostrewa, D.; Berneche, S.; Winkler, F. K.; Li, X.-D. *Proc. Natl. Acad. Sci. U.S.A.* **2004**, *101*, 17090.

(3) Basch, H.; Krauss, M.; Stevens, W. J. *J. Am. Chem. Soc.* **1985**, *107*, 7267.

(4) O'Malley, P. J. *J. Am. Chem. Soc.* **1998**, *120*, 11732.

(5) Machado, F. B. C.; Davidson, E. R. *J. Chem. Phys.* **1992**, *97*, 1881.

(6) Scheiner, S.; Yi, M. *J. Phys. Chem.* **1996**, *100*, 9235.

(7) Tatara, W.; Wojcik, M. J.; Lindgren, J.; Probst, M. *J. Phys. Chem. A* **2003**, *107*, 7827.

(8) Perchard, C.; Novak, A. *J. Chem. Phys.* **1968**, *48*, 3079.

(9) Colombo, L.; Bleckmann, P.; Schrader, B.; Schneider, R.; Plesser, T. *J. Chem. Phys.* **1974**, *61*, 3270.

(10) Loeffen, P. W.; Pettifer, R. F.; Fillaux, F.; Kearley, G. J. *J. Chem. Phys.* **1995**, *103*, 8444.

(11) Su, C. C.; Chang, H. C.; Jiang, J. C.; Wei, P. Y.; Lu, L. C.; Lin, S. H. *J. Chem. Phys.* **2003**, *119*, 10753.

(12) Hockridge, M. R.; Robertson, E. G.; Simons, J. P. *Chem. Phys. Lett.* **1999**, *302*, 538.

(13) Choi, M. Y.; Miller, R. E. *Phys. Chem. Chem. Phys.* **2005**, *7*, 3565.

(14) Schiedt, J.; Weinkauf, R.; Neumark, D. M.; Schlag, E. W. *Chem. Phys.* **1998**, *239*, 511.

(15) Terpstra, P. A.; Otto, C.; Greve, J. *J. Chem. Phys.* **1996**, *106*, 846.

(16) Ilich, P.; Hemann, C. F.; Hille, R. *J. Phys. Chem. B* **1997**, *101*, 10923.

(17) Graindourze, M.; Grootaers, T.; Smets, J.; Zeegers-Huyskens, Th.; Maes, G. *J. Mol. Struct.* **1991**, *243*, 37.

(18) Smedarchina, Z.; Siebrand, W.; Fernandez-Ramos, A.; Gorb, L.; Leszczynski, J. *J. Chem. Phys.* **2000**, *112*, 566.

(19) Gee, M.; Bourdaa, M. H.; Tao, F. M. *Book of Abstracts*, 217th National Meeting of the American Chemical Society, Anaheim, CA, March 21−25, 1999; American Chemical Society: Washington, DC, 1999.

(20) Gorb, L.; Leszczynski, J. *J. Am. Chem. Soc.* **1998**, *120*, 5024.

(21) Gorb, L.; Leszczynski, J. *Int. J. Quantum Chem.* **1998,** *70*, 855.

(22) Sobolewski, A. L.; Adamowicz, L. *J. Chem. Phys.* **1995**, *102*, 5708.

(23) Gorb, L.; Leszczynski, J. *Int. J. Quantum Chem.* **1998**, *70*, 855.

(24) Nagy, P. I.; Durant, G. J.; Smith, D. A. *J. Am. Chem. Soc.* **1993**, *115*, 2912.

(25) Fritscher, J. *Phys. Chem. Chem. Phys.* **2004**, *6*, 4950.

(26) Hummer, G.; Pratt, L. R.; Garcia, A. E. *J. Phys. Chem. A* **1998**, *102*, 7885.

(27) Torrent, M.; Musaev, D. G.; Morokuma, K.; Ke, S. C.; Warncke, K. *J. Phys. Chem. B* **1999**, *103*, 8618.

(28) van Bael, M. K.; Smets, J.; Schoone, K.; Houben, L.; McCarthy, W.; Adamowicz, L.; Nowak, M. J.; Maes, G. *J. Phys. Chem. A* **1997**, *101*, 2397.

(29) Carles, S.; Lecomte, F.; Schermann, J. P.; Desfrancois, C. *J. Phys. Chem. A* **2000**, *104*, 10662.

(30) Talbot, F. O.; Simons, J. P. *Eur. Phys. J. D* **2002**, *20*, 389.

(31) Hartmann, M.; Miller, R. E.; Toennies, J. P.; Vilesov, A. F. *Science* **1996**, *272*, 1631.

(32) Hartmann, M.; Miller, R. E.; Toennies, J. P.; Vilesov, A. F. *Phys. Rev. Lett.* **1995**, *75*, 1566.

(33) Lehmann, K. K.; Scoles, G. *Science* **1998**, *279*, 2065.

(34) Nauta, K.; Miller, R. E. *Science* **2000**, *287*, 293.

(35) Nauta, K.; Miller, R. E. *Science* **1999**, *283*, 1895.

(36) Brink, D. M.; Stringari, S. *Z. Phys. D* **1990**, *15*, 257.

(37) Choi, M. Y.; Dong, F.; Miller, R. E. *Philos. Trans. R. Soc. A* **2005**, *363*, 393.

(38) Choi, M. Y.; Miller, R. E. *J. Am. Chem. Soc.* **2006**, *128*, 7320.

(39) Heath, J. R.; Zhang, Q.; O'Brien, S. C.; Curl, R. F.; Kroto, H. W.; Smalley, R. E. *J. Am. Chem. Soc.* **1987**, *109*, 359.

(40) Nauta, K.; Miller, R. E. *Phys. Rev. Lett.* **1999**, *82*, 4480.

(41) Miller, R. E. *SPIE Proc.* **1998**, *3271*, 151.

(42) Nauta, K.; Moore, D. T.; Stiles, P. L.; Miller, R. E. *Science* **2001**, *292*, 481.

(43) Dong, F.; Miller, R. E. *Science* **2002**, *298*, 1227.

(44) Nauta, K.; Miller, R. E. *J. Chem. Phys.* **1999**, *111*, 3426.

(45) Knuth E. L.; Schilling, B.; Toennies, J. P. *Proceedings of the 19th International Symposium on Rarefied Gas Dynamics. On Scaling Parameters for Predicting Cluster Sizes in Free Jets*; Anonymous Oxford University Press: Oxford, U.K., 1995; Vol. 19, pp 270−276.

(46) Nauta, K. Ph.D. Thesis, University of North Carolina at Chapel Hill, 2000.

(47) Miller, R. E. *Faraday Discuss.* **2001**, *118*, 1.

(48) Toennies, J. P.; Vilesov, A. F. *Angew. Chem., Int. Ed.* **2004**, *43*, 2622.

(49) Chakravorty, K. K.; Parker, D. H.; Bernstein, R. B. *Chem. Phys.* **1982**, *68*, 1.

(50) Stienkemeier, F.; Bunermann, O.; Mayol, R.; Ancilotto, F.; Barranco, M.; Pi, M. *Phys. Rev. B* **2004**, *70*, 214508.

(51) Scoles, G. *Int. J. Quantum Chem.* **1990**, *24*, 475.

(52) Dalfovo, F. *Z. Phys. D* **1994**, *29*, 61.

(53) Schneider, K.; Kramper, P.; Schiller, S.; Mlynek, J. *Opt. Lett.* **1997**, *22*, 1293.

(54) Schneider, K.; Kramper, P.; Mor, O.; Schiller, S.; Mlynek, J. *OSA Trends Opt. Photonics Ser.* **1998**, *19 (Advanced Solid State Lasers)*, 256.

(55) Jucks, K. W.; Miller, R. E. *J. Chem. Phys.* **1987**, *87*, 5629.

(56) Block, P. A.; Bohac, E. J.; Miller, R. E. *Phys. Rev. Lett.* **1992**, *68*, 1303.

(57) Wu, M.; Bemish, R. J.; Miller, R. E. *J. Chem. Phys.* **1994**, *101*, 9447.

(58) Bemish, R. J.; Chan, M. C.; Miller, R. E. *Chem. Phys. Lett.* **1996**, *251*, 182.

(59) Moore, D. T.; Oudejans, L.; Miller, R. E. *J. Chem. Phys.* **1999**, *110*, 197.

(60) Kong, W.; Bulthuis, J. *J. Phys. Chem. A* **2000**, *104*, 1055.

(61) Kong, W. *Int. J. Mod. Phys. B* **2001**, *15*, 3471.

(62) Franks, K. J.; Li, H. Z.; Kong, W. *J. Chem. Phys.* **1999**, *110*, 11779.

(63) Castle, K. J.; Abbott, J.; Peng, X.; Kong, W. *J. Chem. Phys.* **2000**, *113*, 1415.

(64) Callegari, C.; Lehmann, K. K.; Schmied, R.; Scoles, G. *J. Chem. Phys.* **2001**, *115*, 10090.

(65) Douberly, G. E.; Miller, R. E. *J. Phys. Chem. B* **2003**, *107*, 4500.

(66) Frisch, M. J.; Trucks, G. W.; Schlegel, H. B.; Scuseria, G. E.; Robb, M. A.; Cheeseman, J. R.; Montgomery, J. J. A.; Vreven, T.; Kudin, K. N.; Burant, J. C.; Millam, J. M.; Iyengar, S. S.; Tomasi, J.; Barone, V.; Mennucci, B.; Cossi, M.; Scalmani, G.; Rega, N.; Petersson, G. A.; Nakatsuji, H.; Hada, M.; Ehara, M.; Toyota, K.; Fukuda, R.; Hasegawa, J.; Ishida, M.; Nakajima, T.; Honda, Y.; Kitao, O.; Nakai, H.; Klene, M.; Li, X.; Knox, J. E.; Hratchian, H. P.; Cross, J. B.; Adamo, C.; Jaramillo, J.; Gomperts, R.; Stratmann, R. E.; Yazyev, O.; Austin, A. J.; Cammi, R.; Pomelli, C.; Ochterski, J. W.; Ayala, P. Y.; Morokuma, K.; Voth, G. A.; Salvador, P.; Dannenberg, J. J.; Zakrzewski, V. G.; Dapprich, S.; Daniels, A. D.; Strain, M. C.; Farkas, O.; Malick, D. K.; Rabuck, A. D.; Raghavachari, K.; Foresman, J. B.; Ortiz, J. V.; Cui, Q.; Baboul, A. G.; Clifford, S.; Cioslowski, J.; Stefanov, B. B.; Liu, G.; Liashenko, A.; Piskorz, P.; Komaromi, I.; Martin, R. L.; Fox, D. J.; Keith, T.; Al-Laham, M. A.; Peng, C. Y.; Nanayakkara, A.; Challacombe, M.; Gill, P. M. W.; Johnson, B.; Chen, W.; Wong, M. W.; Gonzalez, C.; Pople, J. A. *Gaussian 03*, Revision C.02; Gaussian, Inc.: Wallingford CT, 2004**.**

(67) Choi, M. Y.; Douberly, G. E.; Falconer, T. M.; Lewis, W. K.; Lindsay, C. M.; Merritt, J. M.; Stiles, P. L.; Miller, R. E. *Int. Rev. Phys. Chem.* **2006**, *25*, 15.

(68) Carney, J. R.; Hagemeister, F. C.; Zwier, T. S. *J. Chem. Phys.* **1998**, *108*, 3379.

(69) Eichenauer, D.; Le Roy, R. J. *J. Chem. Phys.* **1988**, *88*, 2898.

(70) Kang, C.; Korter, T. M.; Pratt, D. W. *J. Chem. Phys.* **2005**, *122*, 174301/1.

(71) Florio, G. M.; Zwier, T. S.; Myshakin, E. M.; Jordan, K. D.; Sibert, E. L. *J. Chem. Phys.* **2003**, *118*, 1735.

(72) Nauta, K.; Moore, D. T.; Miller, R. E. *Faraday Discuss.* **1999**, *113*, 261.

(73) Lindsay, C. M.; Douberly, G. E.; Miller, R. E. *J. Mol. Struct.* **2006**, *786*, 96.

(74) Choi, M. Y.; Miller, R. E. Manuscript in preparation.